Physiological Measurement

PAPER • **OPEN ACCESS**

Pulse wave analysis as a tool for the evaluation of resuscitation therapy in septic shock

To cite this article: Riccardo Campitelli *et al* 2023 *Physiol. Meas.* **44** 105002

IOP Publishing Physiol. Meas. 44 (2023) 105002 https://doi.org/10.1088/1361-6579/acfc94

Physiological Measurement

IPEM Institute of Physics and Engineering in Medicine

OPEN ACCESS

RECEIVED
22 June 2023

REVISED
11 September 2023

ACCEPTED FOR PUBLICATION
22 September 2023

PUBLISHED
13 October 2023

PAPER

Pulse wave analysis as a tool for the evaluation of resuscitation therapy in septic shock

Riccardo Campitelli[1], **Manuela Ferrario**[1], **Fuhong Su**[2,3], **Jacques Creteur**[2,3], **Antoine Herpain**[2,4] and **Marta Carrara**[1]

[1] Department of Electronics, Information, and Bioengineering, Politecnico di Milano, Milan, Italy
[2] Experimental Laboratory of Intensive Care, Université Libre de Bruxelles, Brussels, Belgium
[3] Department of Intensive Care, Erasme Hospital, ULB, Brussels, Belgium
[4] Intensive care department, St-Pierre University Hospital, Brussels, Belgium

E-mail: marta.carrara@polimi.it

Keywords: pulse wave analysis, septic shock, cardiovascular modelling, resuscitation protocols, arterial blood pressure waveform

Supplementary material for this article is available online

Abstract

Objective. Pulse wave analysis (PWA) can provide insights into cardiovascular biomechanical properties. The use of PWA in critically ill patients, such as septic shock patients, is still limited, but it can provide complementary information on the cardiovascular effects of treatment when compared to standard indices outlined in international guidelines. Previous works have highlighted how sepsis induces severe cardiovascular derangement with altered arterial blood pressure waveform morphology and how resuscitation according to standard haemodynamic targets is not able to restore the physiological functioning of the cardiovascular system. The aim of this work is to test the effectiveness of PWA in characterizing arterial waveforms obtained from a swine experiment involving polymicrobial septic shock and resuscitation with different drugs. *Methods*. During the experiment, morphological aortic waveform features, such as indices related to the dicrotic notch and inflection point, were extracted by means of PWA techniques. Finally, all the PWA indices were used to compute a clustering classification (mini batch K-means) of the pigs according to the different phases of the experiment. This analysis aimed to test if PWA features alone could be used to distinguish between the different responses to the administered therapies. *Results*. The PWA indices highlighted different cardiovascular conditions of the pigs in response to different treatments, despite the mean haemodynamic values typically used to guide therapy administration being similar in all animals. The clustering algorithm was able to distinguish between the different phases of the experiment and the different responses of the animals based on the unique information derived from the aortic PWA. *Conclusion*. Even when used alone, PWA indices were highly informative when assessing therapy responses in cases of septic shock. *Significance*. A complex pathological condition like septic shock requires extensive monitoring without neglecting important information from commonly measured signals such as arterial blood pressure. Future studies are needed to understand how individual differences in the response to therapy are associated with different cardiovascular conditions that may become specific therapy targets.

1. Introduction

The morphological characteristics of arterial pressure and flow waveform represent an important source of information about the cardiovascular system and they can be investigated to uncover insights into disease processes and therapies (Nichols *et al* 2011). The pulse wave generated by the left ventricle travels away from the heart and is partially reflected at many locations, where changes in geometry and impedance occur; therefore, both pressure and flow waves consist of forward and reflected (or backward) components (Westerhof *et al* 1972).

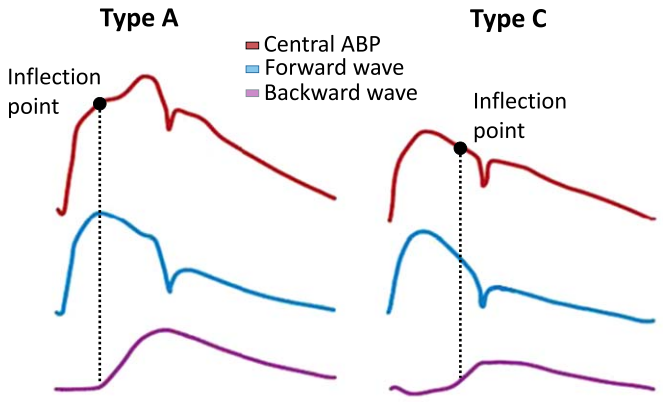

Figure 1. Illustration of type A and type C arterial blood pressure (ABP) waveforms. The red line represents the ABP, the blue and purple lines are the forward and backward waves, respectively. Note that ABP is the sum of the two.

The typical central pressure waveform exhibits a characteristic inflection point during systole (figure 1, left). The initial pressure upstroke until this inflection point is related to the forward travelling wave, i.e. mainly the interaction between flow ejected from the heart and the proximal aorta (characteristic impedance, Zc) (Westerhof and Westerhof 2017). The pressure increase following the inflection point, whose range is called augmented pressure, reflects instead the contribution from the first reflected waves. The timing and amount of wave reflection determine the shape of the arterial pulse. Figure 1 shows two typical waveform types: type A, where the backward waves arrive early during systole and contribute to the rise of systolic pressure and, hence, the increase of cardiac afterload; and type C, where the backward waves arrive later after the systolic peak and contribute more to the myocardial perfusion gradient in the coronary arteries (Nichols *et al* 2011, Westerhof and Westerhof 2012).

Changes in cardiovascular properties, such as large artery stiffness, peripheral resistance, microvascular properties, cardiac contractility and heart rate (HR), all influence the pattern of pressure/flow waves measured in blood vessels. Therefore, analysis of pulse morphology, called pulse wave analysis (PWA), allows an exploration of the biomechanical properties of the cardiovascular system and to derive important information on, among other factors, ventricular efficiency, afterload and ventriculo–arterial coupling, aortic recoil, and vascular tone (Sharman *et al* 2009, Heffernan *et al* 2010, Heusinkveld *et al* 2019, Pagoulatou *et al* 2021). Of note, from a haemodynamic monitoring standpoint, PWA has the capacity to provide insights into the disparity between the measured pressure wave and the flow wave; restoration of blood flow and organ perfusion is the real goal of cardiovascular resuscitation, but blood pressure is most frequently monitored due to the technical constraints associated with obtaining reliable arterial flow measurements in clinical practice.

Numerous clinical studies have shown that PWA can provide valuable prognostic information about traditional risk factors for chronic cardiovascular disease, e.g. diabetes, hypertension, chronic heart failure and chronic kidney disease (Manisty *et al* 2010, Chirinos *et al* 2012, Zamani *et al* 2014).

In the intensive care unit (ICU), acute critically ill patients may be subject to profound alterations of cardiac and arterial properties. In addition, the necessary clinical interventions to prevent life-threating events, e.g. drug administration, organ support and fluid infusion, may further contribute to these alterations. For example, norepinephrine, the first-line vasopressor used in ICUs, has been proven to modify arterial pressure propagation and reflection phenomena, affecting left ventricular efficiency, in a septic shock population (Monge García *et al* 2018). Septic shock is one of the leading causes of mortality in the ICU, with a hospital mortality rate approaching 40% (Singer *et al* 2016, Rudd *et al* 2020). It is characterized by severe hypotension and hypovolemia caused by massive vasodilation and capillary leakage triggered by systemic inflammation (Landry and Oliver 2001, Cecconi *et al* 2018). The consequent reduction in stroke volume (SV) leads to a decrease in cardiac output (CO) and thus to tissue hypoperfusion, elicitinga remarkable compensatory adrenergic stimulus by increasing HR and ventricular contractility (Cecconi *et al* 2018). Current clinical guidelines for septic shock resuscitation recommend the administration of antibiotics, fluids and vasopressors; in particular, norepinephrine as first choice. The objective isto restore blood pressure and circulating volume, aiming for a mean arterial pressure (MAP) $\geqslant$ 65 mmHg to guarantee sufficient tissue oxygenation (Evans *et al* 2021). However, reaching the target global haemodynamic stability does not automatically implya return to physiological homeostasis and ventriculo–arterial coupling. Indeed, these cardiovascular alterations often persist and they may be detected by the analysis of the pulse wave characteristics, as previously explained.

Previous results from our group have shown how, in several animal populations undergoing sepsis/septic shock and different resuscitation protocols, reduced arterial compliance, total peripheral resistance and pulse pressure amplification were still present even after standard resuscitation with fluids and vasopressors was evaluated to be successful according to recommended targets. Moreover, the morphological profile of the blood pressure waveform continued to exhibit changes upon completion of the resuscitation protocol, reinforcing the evidence for persistent alterations in the cardiovascular system involving blood pressure propagation and reflection (Carrara *et al* 2020a, 2020b, 2022).

Since PWA provides important indications about the cardiovascular condition, we hypothesized that waveform-derived indices could provide further insights into the cardiovascular response to treatments administered in the ICU. For this reason, we investigated changes in arterial waveform morphology by using PWA techniques in combination with standard indices. The objectives were twofold: (i) to test the effectiveness of PWA indices to characterize arterial waveform changes during a relevant experimental model of septic shock, including standard resuscitation care with fluids and noradrenaline; and (ii) to verify the effects of two drugs, esmolol and ivabradine, that are commonly used to reduce the heart rate (HR) and were recently proposed to control septic-induced tachycardia (Morelli *et al* 2015). A persisting high HR despite resuscitation is indeed associated with septic-induced myocardial dysfunction, an independent risk factor for increased mortality (Rudiger and Singer 2013, Morelli *et al* 2015). The mechanism of action of the two drugs is very different: esmolol is a cardioselective β1-adrenoreceptors antagonist, thereby it reduces the HR by blocking the effect of any adrenergic stimuli at the level of the cardiac receptors (Rudiger and Singer 2013); basically, it decreases the force and rate of heart contractions by blocking beta-adrenergic receptors of the sympathetic nervous system, thereby preventing the action of both epinephrine and norepinephrine (also called noradrenaline). Ivabradine specifically inhibits the pacemaker funny current of the sinoatrial node, a mixed sodium–potassium inward current that controls spontaneous diastolic depolarization in the sinoatrial node, and hence regulates the HR; thereby, it affects the HR without acting on any adrenergic receptors and thus on ventricular contractility or vascular tone (Müller-werdan *et al* 2016). Given their different interactions with cardiac functions, we may expect different cardiovascular responses to these drugs; moreover, some experimental evidence indicates that esmolol could exert systemic anti-inflammatory and beneficial effects on vascular tone (Kimmoun *et al* 2015), even if administered at low doses, avoiding the hypotensive side effect (Wei *et al* 2016). Questions remain as to how the administration of these drugs affects the cardiovascular system and what impact they have on long-term sequalae. We believe that PWA could help answer these questions.

2. Material and methods

2.1. Study design and experimental procedure

The experiments were performed in the Experimental Intensive Care Laboratory (LA1230336) at the Université Libre de Bruxelles with the approval of the local ethics committee (Commission d'Ethique et du Bien-Etre Animal - CEBEA (ULB), Protocol number 448N, approval date March 2012), and it was conducted in accordance with the EU Directive 2010/63/EU for animal experiments and the ARRIVE guidelines for animal research. Further details are reported in the supplemental material.

Fifteen pigs of both sexes with weight in the range 39–52 kg were instrumented and successively allowed to rest for ~2 h, after which the first baseline measurements and blood samples were taken (baseline, T1). Sepsis was induced by intraperitoneal instillation of autologous faeces, filtered and diluted in 300 ml of 10% glucose. After the insult, fluid maintenance was limited so that the animal reached a severe condition of hypotension, i.e. MAP = 45÷50 mmHg for 1 h, (septic shock condition, T2). Immediately afterwards, a full fluid resuscitation was initiated by administering crystalloid and colloid to maintain arterial pulse pressure variation $\leqslant$ 12% throughout the entire experiment. The next time point (T3) was settled after 2 h of resuscitation when the animal was considered stable, i.e. with a stable MAP and without further increases in CO. Following fluids resuscitation, the animals were divided into three groups: (i) the ivabradine-treated group (IVB, n = 6); (ii) the esmolol-treated group (ESM, n = 6); and the (iii) the control group (CTR, n = 3). The first two groups received ivabradine or esmolol at incremental doses until the HR was decreased to be in the range of 80–90 bpm and maintained for 1 h. The untreated animals received only fluids during this phase. The end of this period was defined as time point T4. Finally, all the animals received a continuous infusion of norepinephrine with a fixed dose of 0.3 μg Kg^{-1} min^{-1} for 1 h (T5). Euthanasia was then practiced for all animals with an injection of potassium chloride and an overdose of sodium thiopental.

Arterial blood pressure (ABP) in the ascending aorta and left ventricular pressure were continuously recorded during the experiment (5F pressure catheter, Transonic System Europe, The Netherlands, and Pressure-Volume Loop catheter, Transonic System Europe, The Netherlands, respectively); continuous CO was acquired through pulmonary artery catheter (Edwards LifeSciences, California, USA). All acquired signals were

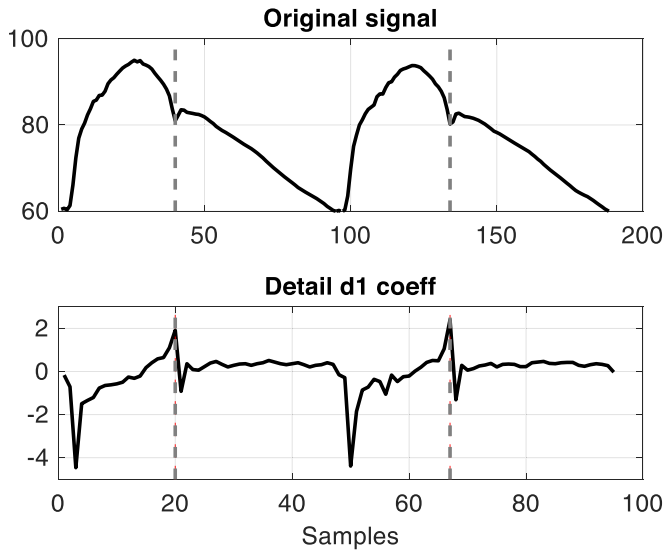

Figure 2. Illustration of dyadic wavelet transform of arterial blood pressure pulse for dicrotic notch detection. Coefficient values d1 are down-sampled by a twofold factor with respect to the original signal (see appendix for further details).

converted using an A/D converter (Notocord Hem, Notocord, France) with high temporal resolution (500 Hz). For each time point, stationary segments (average duration of 15 min) of aortic pressure signal were extracted from the Notocord software and imported into the MATLAB® framework for the analyses.

2.2. Standard arterial pressure features

A flow chart illustrating the data workflow is reported in the supplementary materials (figure S2). Beat-to-beat time series of systolic (SAP), diastolic (DAP) and MAP were obtained from aortic ABP waveforms using standard algorithms (Zong *et al* 2003, Sun *et al* 2004). The time series of arterial pulse pressure (PP) was computed as the difference between SAP and DAP within the same beat. The time series of the heart period (HP) was obtained by computing the time difference between consecutive onsets of ABP and is considered as a surrogate for the RR-interval time series; HR was derived as 60/HP (bpm). The maximum positive time derivative of aortic ABP (*dP/dt* max) was calculated on a beat-to-beat basis from aortic ABP recording. The systolic upstroke time (UT) was calculated as the time interval between SAP occurrence and the onset of the beat. All the beat-to-beat indices were then averaged and considered for successive analyses.

2.3. Semi-automatic algorithm for dicrotic notch identification and indices extraction

The dicrotic notch (DN) appears as a secondary upstroke in the descending part of a pulse trace corresponding to the transient increase in aortic pressure upon closure of the aortic valve; therefore, it marks the end of the ejection phase. While in physiological conditions the DN is highly evident on the waveform, in patients with a compromised cardiovascular system, like critically ill patients, its detection is non-trivial since the pressure signal may greatly deviate from the physiological shape. Typically, conventional methods for DN detection look for the zero crossing of the signal derivatives (Karamanoglu 1997, Li *et al* 2010); however, these methods are highly prone to error in noisy signals or in cases of large alterations in ABP wave morphology.

Wavelet transform has been proposed in the past for the extraction of characteristic features from biological signals, such as ABP or electrocardiogram, with promising results (Antonelli *et al* 1994, Minhas and Arif 2008, Pachauri and Bhuyan 2012).

In this work, we have implemented a first-level dyadic wavelet transform using the Haar wavelet to identify the DN on each ABP beat (Antonelli *et al* 1994). More details about the wavelet theory and the algorithm can be found in appendix. The positive peak of the first-level detail coefficients coincides with the DN on the original signal, after up-sampling, as shown in figure 2.

Two automatic correction algorithms were further implemented to correct the DN identification: (i) an algorithm that looks for the minimum point close to the identified DN (local minima adjustment); (ii) a second algorithm for very smooth ABP signals, similar to a bell shape (e.g. during septic shock) – in this case a sharp incisure is not visible, so the DN is identified as a change in slope during the diastolic decay. The algorithm looks for the closest point to the one identified where the slope of the signal changes considerably (slope change adjustment) (figure 3).

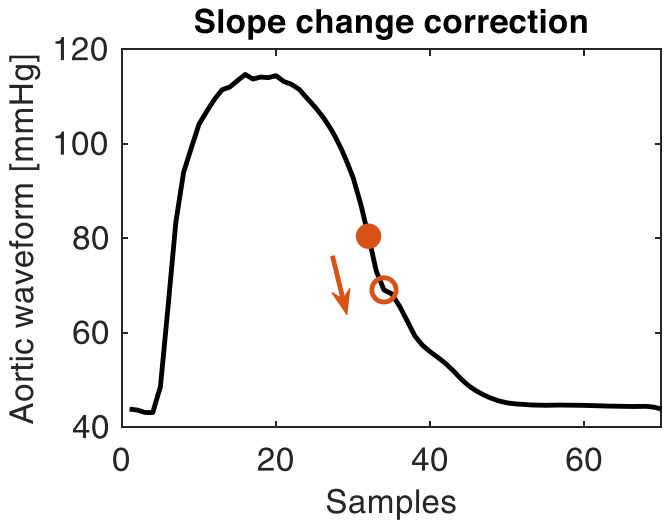

Figure 3. The dicrotic notch originally identified by the algorithm (full circle) is replaced (empty circle) according to the slope change adjustment result.

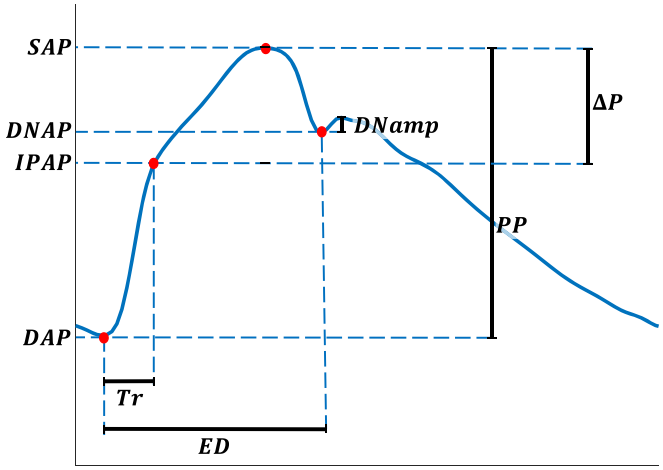

Figure 4. Waveform-derived indices extracted from aortic ABP. SAP: systolic arterial pressure (mmHg); DAP: diastolic arterial pressure (mmHg); PP: pulse pressure (mmHg); DNAP: dicrotic notch arterial pressure (mmHg); DNamp: dicrotic notch amplitude (mmHg); IPAP: inflection point arterial pressure (mmHg); ΔP: augmented pressure (mmHg); ED: ejection duration (s); Tr: time of occurrence of the inflection point, referred to as beat onset (s).

In the supplementary material, we report the results supporting the reliability of the proposed algorithm for DN identification.

Once the DN is identified, several indices can be computed: the DN arterial pressure (DNAP; mmHg), which is the pressure value at the DN; DN amplitude (DNamp; mmHg), calculated as the difference between the value of maximum pressure after the DN and DNAP); ejection duration (ED; s), calculated as the time difference between the beat onset and DN occurrence; and the SAP to DNAP ratio (a.u.], i.e. the ratio between the SAP and DNAP values (figure 4).

2.4. Inflection point detection and wave reflection indices

The inflection point corresponds to the arrival of the backward wave (see figure 1). It is extracted using the method proposed by Karamanoglu (Rudiger and Singer 2013), which is based on signal derivatives. In particular, the inflection point for a type A pulse is identified as the point where the third-order signal derivative crosses the zero from positive to negative values after the dP/dt max point; conversely, for a type C pulse wave, the inflection point is expected to occur where the third-order derivative crosses the zero from negative to positive after the systolic peak. Further details about this algorithm and its performance can be found in the supplementary material.

Once the inflection point was identified, we computed the following indices related to wave reflection (figure 4): (i) the pressure value at the inflection point (IPAP; mmHg); (ii) the augmented pressure (ΔP; mmHg), computed as the difference between the SAP and IPAP values; (iii) the augmentation index (AIx; %), computed as the percentage ratio between ΔP and PP; (iv) the arrival time of the backward wave (Tr; s), obtained as the time delay between ABP upstroke onset and the inflection point (Kelly *et al* 1989, Baksi *et al* 2009). In this study, for each time point, a beat template obtained by averaging 15 beats of the aortic ABP signal was used to identify the inflection point and the derived indices.

2.5. Statistical analyses

The indices computed on a beat-to-beat basis were averaged to have one value at each time point for each animal. The indices related to the inflection point (i.e., inflection point, ΔP, AIx, Tr) were computed using the beat template, as previously explained.

Within-group differences among time points were examined with the Friedman test. In cases where the Friedman test p-value < 0.05, we adopted the Wilcoxon signed-rank test to assess significant changes between pairs of time points within each group of animals. Tukey's honestly significant difference was used to correct the p-value significance. The Kruskal–Wallis test was used at each time point to compare the three groups. If significance was observed, the Mann–Whitney U test was then employed to test the differences among the experimental groups. Significance was considered based on a p-value < 0.05.

2.6. Unsupervised cluster analysis

We hypothesized that the morphological features of the aortic pulse alone are able to distinguish the different responses to the administered therapies and, therefore, to provide some insights into the condition of the cardiovascular system. Indeed, in our previous study (Carrara *et al* 2020b), we found out that from a qualitative visual inspection the aortic waveforms from the three groups were very different after therapy administration. Given the baseline (T1) and shock (T2) conditions as references, as all the animals are similar according to the protocol, we were interested to see how the three experimental groups clustered after the resuscitation manoeuvres and administration of vasopressors.

Unsupervised clustering of the indices at time points T1, T2 and T5 was performed by including only the indices related to the morphology of the aortic waveform described above, i.e. PP, UT, dP/dt max, DNAP, DNamp, ED, SAP/DNAP, IPAP, Tr, ΔP and AIx.

The mini-batch K-means method was used for clustering and principal component analysis was used to display the results. The number of clusters was found by using the silhouette score (Sculley 2010).

3. Results

3.1. Standard haemodynamic indices

Table 1 reports the distribution of mean values of aortic MAP, SAP, DAP and HR at different time points; CO and SV are also reported. As expected, MAP significantly decreased while HR significantly increased after septic shock development at T2. HR remained elevated in the control group until the end of the experiment, whereas in the two groups treated with negative chronotropic agents the HR reached the target ($<$90 bpm) at T4 and remained lower than that of the control group, although significantly in ESM group only. After noradrenaline administration (T5), MAP increased in all animals approaching the threshold of 65 mmHg, but without reaching baseline values. In the ivabradine group, SAP increased so to exceed baseline values. DAP values were lower than baseline in all pigs at the end of resuscitation.

3.2. Waveform-derived indices

Figure 5 shows an example of an aortic ABP waveform registered at baseline (T1), after septic shock development (T2) and at the end of the experiment after haemodynamic resuscitation (T5) for one pig of each experimental group. The waveform of the three pigs changes along with the experiment and are different among the three groups at the end of the experiment (T5). At T2, the aortic waveform has a bell shape, with a smoother trend and less clear incisures compared to T1 in all pigs. At T5, the esmolol pigs showed some morphological features more similar to baseline than the other two groups, e.g. a clearer DN and a more evident inflection point, despite the three pigs having similar MAP values. The indices proposed in this work have been chosen to quantitatively track these changes in the arterial pulse along the experimental protocol.

After septic shock development (T2), the aortic UT values significantly decreased in all pigs compared to baseline, probably related to the shortening of heart-beat duration (figure 6). At T4, the esmolol pigs showed a significant increase of UT, returning to values similar to baseline, and a decrease in dP/dt max.

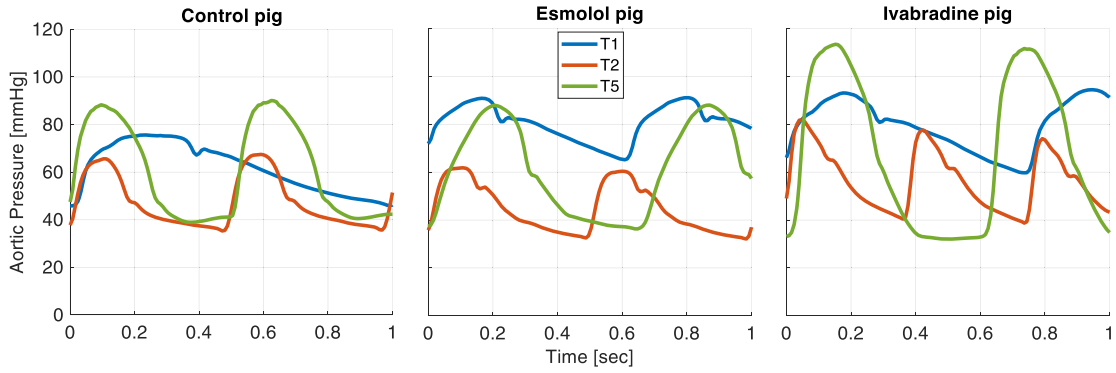

Figure 5. Example of aortic ABP waveform at baseline (T1), after septic shock development (T2) and at the end of the experiment after haemodynamic resuscitation (T5) for one pig of each experimental group.

Table 1. Mean haemodynamic indices computed for aortic blood pressure. Values are reported as median (25th,75th) percentile.

		T1	T2	T3	T4	T5
MAP	CTR	63 (62,73)	45 (44,46)	62 (62,66)	58 (58,61)	62 (60,73)
	ESM	75 (68,80)	45 (38,51)**	61 (52,68)§	55 (48,57)*	61 (57,66)§
	IVB	73 (63,83)	48 (47,50)**	58 (54,63)	54 (52,57)*	66 (55,71)
SAP	CTR	79 (77,87)	62 (60,65)	82 (80,86)	78 (75,81)	90 (89,99)
	ESM	90 (83,94)	65 (58,69)**	86 (80,88)	79 (75,84)	92 (83,95)§§
	IVB	87 (79,97)	69 (64,73)*	80 (76,88)§	82 (77,86)	113 (104,117)
DAP	CTR	52 (48,59)	35 (33,36)	49 (48,50)	45 (44,46)	42 (40,51)
	ESM	59 (54,66)	33 (26,37)**	39 (36,53)§	38 (33,42)*	41 (36,47)
	IVB	56 (47,67)	36 (34,37)**	42 (38,44)	37 (34,38)**	37 (30,45)
HR	CTR	60 (60,81)	122 (118,123)*	113 (113,114)	107 (103,110)	119 (114,140)
	ESM	83 (75,91)	125 (123,140)**	116 (107,123)	87 (83,92)§§	91 (84,92)°°§
	IVB	77 (69,80)	137 (136,151)°**	119 (109,143)*	89 (81,91)°	103 (97,107)
CO	CTR	3.6 (3.5,4.5)	3.3 (3.3,3.3)$^{n=1}$	4.8 (4.6,6.3)	4.4 (4.3,6.2)	6.7 (6.4,8.7)*
	ESM	5.1 (3.8,5.7)	2.9 (2.8,3.2)$^{n=4}$	5.5 (5.2,5.7)	4.2 (4.0,5.4)	5.5 (5.1,5.9)§
	IVB	3.9 (2.7,4.1)	2.2 (2.0,3.0)	4.7 (4.2,7.1)§	4.5 (3.7,5.2)	6.5 (5.7,6.7)$^{n=5}$§§
SV	CTR	57 (55,60)	28 (28,28)$^{n=1}$	43 (41,56)	42 (40,58)	56 (56,62)
	ESM	59 (53,63)	24 (21,26)$^{n=4}$*	47 (45,50)	49 (46,62)	61 (56,64)§
	IVB	49 (47,52)	16 (15,20)	40 (36,45)	50 (47,57)§	64 (57,67)$^{n=4}$§§

MAP: aortic mean arterial pressure (mmHg); SAP: aortic systolic arterial pressure (mmHg); DAP: aortic diastolic arterial pressure (mmHg); HR: heart rate (bpm); CO: cardiac output (L min^{-1}); SV: stroke volume (mL); T1: baseline; T2: after septic shock development; T3: after fluids; T4: after drugs (esmolol/ivabradine); T5: after noradrenaline. Wilcoxon signed test: $^{*}p < 0.05$, $^{**}p < 0.01$ with respect to T1, §p-value < 0.05, §§p-value < 0.01 with respect to T2 (Friedman test p-value < 0.05). Mann–Whitney U test: $^{\circ}p < 0.05$, $^{\circ\circ}p < 0.01$ versus CTR at the specified time point (Kruskal–Wallis test p-value < 0.05).

UT and dP/dt max are highly dependent on left ventricular contractility. Esmolol has β1-adrenergic inhibitory effect, so the trends in these two indexes may be explained as an effect of this drug. In support of this hypothesis, we observed a significant increase in dP/dt max and a significant reduction in UT from T4 to T5 in control and ivabradine pigs only, which was expected as a physiological response to exogenous noradrenaline administration, which encompasses some β1-agonist effects. The aortic PP was significantly elevated in all pigs at T5 with respect to baseline, with the ivabradine pigs showing the highest values, proportionally to the highest increase in SV observed from T4 to T5 in that group.

The DNAP trend was similar in all groups, with a significant decrease at T2, consistent with the overall decrease in vascular tone induced by septic shock, and a partial restoration after resuscitation (T5), although without reaching baseline values. The values of DNamp decreased from T1 to T2 in all pigs and remained significantly lower than baseline until the end of the experiment. Interestingly, at T5, DNamp values in the control and ivabradine groups were very close to zero. In contrast, the esmolol population values were higher; this could be potentially related to a better aortic wall recoil and/or more reflection of the backward waves in early diastole.

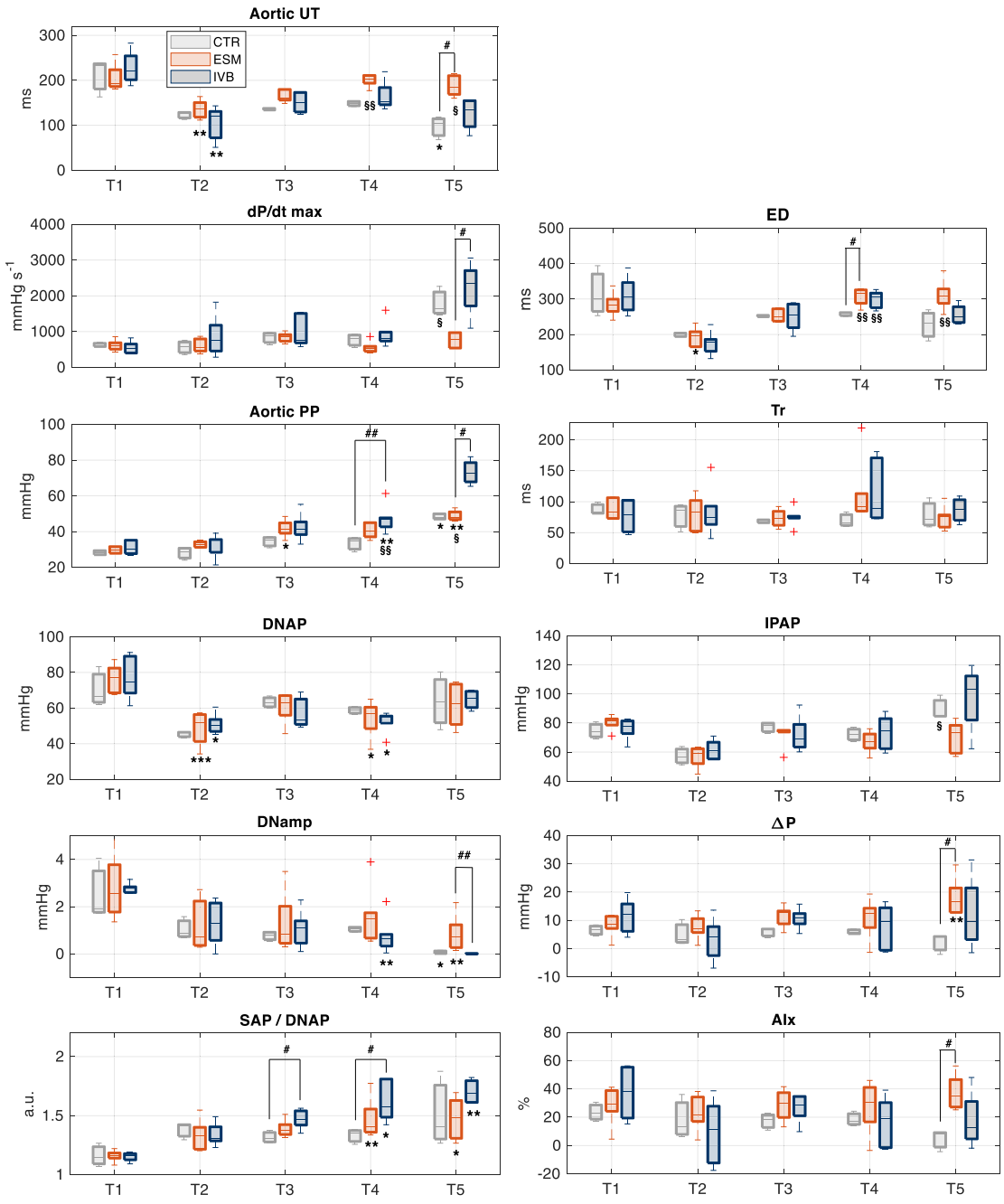

Figure 6. Boxplots of aortic waveform-derived indices. UT: upstroke time; *dP*/*dt* max: maximum steepness of aortic systolic upstroke; PP: pulse pressure; DNAP: dicrotic notch arterial pressure; DNamp: dicrotic notch amplitude; SAP: systolic arterial pressure; ED: ejection duration; Tr: time of occurrence of the inflection point; IPAP: inflection point arterial pressure; ΔP: augmented pressure; AIx: augmentation index; T1: baseline; T2: septic shock; T3: after fluids; T4: after drugs; T5: after noradrenaline. Wilcoxon signed test: $^{*}p < 0.05$, $^{**}p < 0.01$, $^{***}p < 0.001$ with respect to T1, §p-value < 0.05, §§p-value < 0.01 with respect to T2 (Friedman test p-value < 0.05). Mann–Whitney U test: $\#p < 0.05$, $\#\#p < 0.01$ between the two groups, the significant comparisons are highlighted by the lines (Kruskal–Wallis test p-value < 0.05).

The trend of ejection duration (ED) values was in agreement with the HR trend. The administration of a vasopressor at T5 had no effects on ED in the esmolol group, but the other two groups showed a further reduction in their ED values due to the adrenergic stimulation, i.e. a shortening in ED. Finally, the SAP/DNAP ratios showed an increasing trend during the overall experiment in all pigs, without returning to baseline values. The ivabradine group was characterized by the highest values, driven by the higher values of aortic SAP.

The values of IPAP decreased from T1 to T2 in all animals, consistent with the overall trend of blood pressure values. After administration of noradrenaline (T5), the ivabradine and the control groups only showed a further increase in IPAP values. only at T5 the values of AIx did not show significant changes during the experiment. It was only at T5 that the esmolol group exhibited higher values compared to the other groups and values more

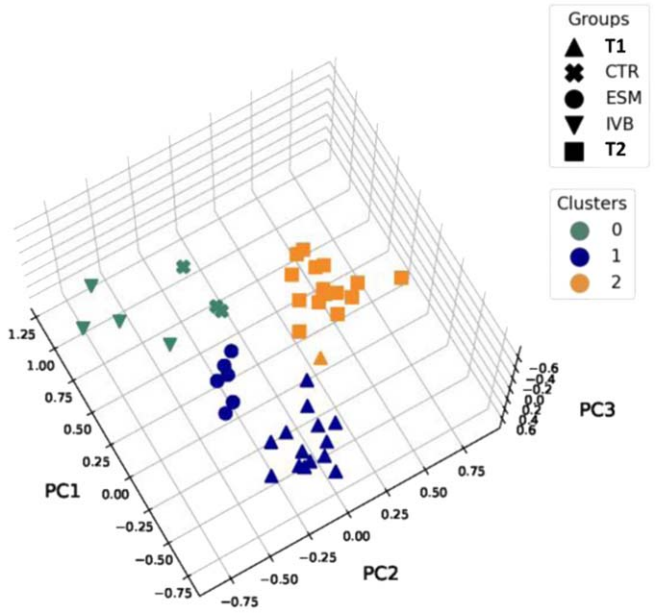

Figure 7. Results of the mini-batch K-means algorithm. The triangle represents all animals at baseline (T1), the square represents all animals during septic shock phase (T2), the cross represents the control pigs (CTR) at the end of experiment (T5), the circle represents the esmolol pigs (ESM) at T5, and the downward triangle represents the ivabradine pigs (IVB) at T5. PC: principal component.

similar to baseline. This result can be explained by a larger augmented pressure (ΔP) and lower IPAP values with respect to the other groups. In the control group, the AIx values were lower mainly due to very low ΔP values. Whereas in the ivabradine group the values of AIx were slightly lower mainly for the larger aortic PP values. There were no significant differences in Tr values among the groups and during the experiment.

3.3. Clustering

Figure 7 shows the results of the mini-batch K-means clustering analysis. The first three PCA components are displayed, as they guarantee a percentage of variance explained as $>$ 80% of the total variance. The optimal number of clusters was 3 based on the silhouette score. The result shows that the indices related to arterial waveform grouped the pigs according to the epochs of the experiments as expected: baseline (T1, triangles) and septic shock (T2, squares) pigs were placed in two separate clusters (only one animal misclassified), i.e. cluster 1 and cluster 2. All esmolol pigs at T5 (blue circles) were included in cluster 1 together with the pigs at baseline. Finally, all the ivabradine and control pigs at T5 (green downward triangles and crosses, respectively) were grouped in a separate cluster (cluster 0) – their features could be considered neither similar to baseline nor to septic shock condition.

4. Discussion and conclusion

Sepsis and septic shock are known to severely impair cardiovascular function, leading to altered pulse wave characteristics and transmission along the arterial tree. Current clinical guidelines for septic shock resuscitation mainly concern restoring mean haemodynamic targets, such as blood pressure and blood flow to tissues using conventional thresholds such as MAP $>$ 65 mmHg (Evans *et al* 2021). However, morphological alterations of the arterial waveform are typically overlooked during resuscitation, despite they can be highly informative regarding the underlying cardiovascular functions and properties. Previous works on experimental septic shock have shown how the arterial waveform still exhibits an evident morphological alteration despite successful haemodynamic resuscitation, hinting that the recovery of mean haemodynamic targets does not directly imply the return to a physiological condition (Carrara *et al* 2020a, 2022).

In this study, we showed the potential of arterial waveform-derived indices in detecting the arterial response during an experimental protocol of polymicrobial septic shock development and resuscitation with different chronotropic drugs. As shown in figure 5, all pigs display an aortic waveform with a bell shape during shock (T2), with a smoother trend and less clear incisures compared to baseline. Theoretically, a 'flatter' pulse wave is a sign of reduced wave reflection, consistent with the typical condition of peripheral vasodilation and vasoplegia (Cecconi *et al* 2018). The DN morphology is also highly dependent on the reflected waves; for example, a decline

of peripheral resistance can cause the delay in the arrival time of the reflected wave so that the forward wave hides it and the DN becomes negligible (Nichols *et al* 2008) with DNamp values close to 0 (see figure 6).

During shock, we also found decreased UT values suggesting a faster rise during the systolic phase, supporting a stiffening of the arterial vessels and/or a loss of vascular tone, as already widely reported in the literature (Hatib *et al* 2011, Joffre *et al* 2020, Carrara *et al* 2020a).

The AIx values did not show a consistent trend in all animals after septic shock development. Peripheral vasodilation and reduced wave reflections would have suggested a marked decrease in AIx values. However, this index reflects complex interactions and depends not only on the amount and timing of backward waves but also on the PP, which is in turn driven by the interplay between aortic compliance and SV. The interpretation of this index is very difficult if the other factors change concurrently. In healthy conditions, we know that HR affects AIx (Wilkinson *et al* 2002) and an increase in HR causes a decrease in AIx, mainly due to the earlier arrival of the next beat that is superimposed on the reflected waves. The same mechanism may also explain the decrease in AIx observed in healthy individuals during peripheral vasodilation (Kelly *et al* 2001, Pauca *et al* 2005) and during β1-adrenergic stimulation, where the decrease in AIx is probably related to the increase in HR rather than to an increase in cardiac contractility (Sharman *et al* 2009). In contrast, noradrenaline stimulation has been shown to increase AIx due to the greater amount of wave reflections related to the peripheral vasoconstriction (Monge García *et al* 2018).

Moreover, the other component in AIx computation, i.e. aortic PP, is also independently altered by septic shock. In fact, aortic PP is proportional to SV and inversely related to the arterial compliance (Dart and Kingwell 2001). During septic shock, the SV is highly reduced due to the hypovolemic condition, but the aortic PP values remain almost unchanged compared to baseline (table 1). This may be explained by a reduction in aortic compliance, as reported in previous studies from our group (Carrara *et al* 2020a, 2020b) and from others highlighting a stiffening of central vessels in response to acute inflammation (Vlachopoulos *et al* 2005) and sepsis (Hatib *et al* 2011). A stiffer arterial system alters the speed of the pulse wave along the arterial tree, thereby influencing the reflected waves and, consequently, the AIx value.

In our swine population, as well as in critically ill subjects, several factors were changing at the same time and these can explain the high variability in AIx values. Therefore, AIx should be used with caution in an ICU context.

After resuscitation at T5, the arterial pulse of the three pigs appeared to be very different (figure 5), despite similar mean values of traditional haemodynamic variables (table 1). In particular, the esmolol group was found to have a waveform more similar to baseline, with slower systolic rise (UT and dP/dt max) and diastolic decay, and a clearer DN (DNamp). The values of AIx were higher and more similar to baseline values in esmolol pigs compared to the other two populations. This may be a result of the reduced HR, the decreased adrenergic stimulation at the heart level and, probably, an improved vascular condition of the arterial tree, i.e. higher peripheral resistance and lower aortic stiffness (Carrara *et al* 2020b), which can in turn affect pulse wave velocity.

As regards the clustering analysis, we were interested to study how the three experimental groups were grouped after the resuscitation manoeuvres and vasopressor administration on the basis of morphological features of the aortic pulse alone. The result of the mini-batch K-means algorithm showed how the esmolol pigs at T5 were included in the cluster containing all the baseline animals, whereas the ivabradine and control pigs at T5 were included in a separate cluster. After the administration of a cardioselective β1-receptor blocker and noradrenaline, the pigs were characterized by an arterial waveform similar to baseline, possibly suggesting a condition of blood flow propagation and less altered cardiovascular interactions, despite all animals receiving successful haemodynamic resuscitation and achieving the standard targets according to international guidelines.

4.1. Limitations of the study

The limited sample size of the three populations may have affected the statistical results. In addition, no measure of blood flow was available, so indexes describing the forward and backward waves separately could not be computed. Future studies including measures of the blood flow and in larger populations could be useful to generalize the present results. The relation of these findings with long-term outcomes still needs to be investigated.

4.2. Conclusion

The indexes derived from the arterial waveform proved to be highly informative, even when used alone in a study of therapy response in septic shock. They provided important insights into the cardiovascular condition that are not achieved by the standard haemodynamic monitoring commonly used according to standard care for septic shock resuscitation. Indeed, the same MAP value in two different subjects can hide two different cardiovascular conditions or can be achieved by very different therapeutic strategies. In this work, for example, septic-induced tachycardia was reduced by means of two drugs with different mechanisms of action: esmolol, a

cardioselective β1-blocker, and ivabradine, a pacemaker funny current inhibitor. The aortic waveform at the end of the protocol was different, but static haemodynamic indices like MAP were pretty similar.

A complex pathological condition like septic shock requires extensive monitoring without neglecting important information from routinely measured signals such as ABP. Future studies are necessary to understand how the individual differences in the response to the therapy are associated with different cardiovascular conditions, which may help in tailoring the therapy.

Data availability statement

The data cannot be made publicly available upon publication because the cost of preparing, depositing and hosting the data would be prohibitive within the terms of this research project. The data that support the findings of this study are available upon reasonable request from the authors.

Appendix

Generally, the wavelet transform of a continuous signal $x(t)$ is given by

$$X_w(a,\, b) = \frac{1}{\sqrt{a}} \int_{-\infty}^{+\infty} x(t)\psi\left(\frac{t-b}{a}\right) \tag{A1}$$

where a is the scale parameter ($a>0$), b is the translation parameter, used to shift and localize the wavelet function in time, and $\psi\left(\frac{t-b}{a}\right)$ is the shifted and scaled version of a mother wavelet which is used as a basis for wavelet decomposition of the input signal. Low values of a enable to localize fast transitions, whereas higher values localize coarser changes. If the wavelet $\psi(t)$ is the derivative of a smoothing function $\theta(t)$, it can be demonstrated that the wavelet transform of the signal $x(t)$ at scale a is

$$X_w(a,\, b) = -a\left(\frac{d}{db}\right) \int_{-\infty}^{\infty} x(t)\theta_a(t-b)dt \tag{A2}$$

where $\theta_a(t) = \left(\frac{1}{\sqrt{a}}\right)\theta\left(\frac{t}{a}\right)$ is the smoothing function scaled of factor a (Mallat and Zhong 1992, Pachauri and Bhuyan 2012).

It is evident from the above equation that the wavelet transform at scale a is proportional to the derivative of the original signal filtered with a smoothing impulse response at scale a. Therefore, local maxima or minima of the smoothed signal will occur on the zero crossings of the wavelet transform at different scales, and the wavelet modulus maxima detection allows us to find the signal sharp variation points. If the scale and translation parameters are discretized such that $a = 2^k$ and $b = 2^k l$, the transform is then called the dyadic wavelet transform with basis functions

$$\psi_{k,l}(t) = 2^{-\frac{k}{2}}\psi(2^{-k}t - l) \quad k,\, l \in \mathbb{Z}^+. \tag{A3}$$

The dyadic wavelet transform can be implemented as a cascade of high-pass and low-pass filters derived from the mother wavelet. The outputs of high-pass and low-pass filters consist, respectively, of a detailed signal of small-scale information and of an average signal of large-scale information from the original signal. The average signal can undergo subsampling to generate another new detailed signal and average signal. Thus, the dyadic discrete wavelet transform contains the dilated and translated form of the mother wavelet.

References

Antonelli L, Ohley W and Khamlach R 1994 Dicrotic notch detection using wavelet transform analysis *Ann.Int. Conf. IEEE Eng. Med. Biol. Proceedings of 16th Annual International Conference of the IEEE Engineering in Medicine and Biology Society, Baltimore, MD, USA* vol 2, pp 1216–7

Baksi A J *et al* 2009 A meta-analysis of the mechanism of blood pressure change with aging *J. Am. Coll. Cardiol.* **54** 2087–92

Carrara M *et al* 2022 Autonomic and circulatory alterations persist despite adequate resuscitation in a 5-day sepsis swine experiment *Sci. Rep.* **12** 1–14

Carrara M, Herpain A, Baselli G and Ferrario M 2020a Vascular decoupling in septic shock: the combined role of autonomic nervous system, arterial stiffness, and peripheral vascular tone *Front. Physiol.* **11** 1–13

Carrara M, Niccolo A, Herpain A and Ferrario M 2020b Reducing tachycardia in septic shock patients: Do esmolol and ivabradine have a chronotropic effect only? *Proc. Annu Int. Conf. IEEE Eng. Med. Biol. Soc. EMBS* **2020** 382–5

Cecconi M, Evans L, Levy M and Rhodes A 2018 Sepsis and septic shock *Lancet* **392** 75–87

Chirinos J A *et al* 2012 Arterial wave reflections and incident cardiovascular events and heart failure: MESA (Multiethnic Study of Atherosclerosis) *J. Am. Coll. Cardiol.* **60** 2170–7

Dart A M and Kingwell B A 2001 Pulse pressure—a review of mechanisms and clinical relevance *J. Am. Coll. Cardiol.* **37** 975–84

Evans L *et al* 2021 Surviving sepsis campaign: international guidelines for management of sepsis and septic shock 2021 *Intensive Care. Med.* **47** 1181–247

Hatib F, Jansen J R C and Pinsky M 2011 Peripheral vascular decoupling in porcine endotoxic shock *J. Appl. Physiol.* **111** 853–60
Heffernan K S, Patvardhan E A, Hession M, Ruan J, Karas R H and Kuvin J T 2010 Elevated augmentation index derived from peripheral arterial tonometry is associated with abnormal ventricular-vascular coupling *Clin. Physiol. Funct. Imaging* **30** 313–7
Heusinkveld M H G *et al* 2019 Augmentation index is not a proxy for wave reflection magnitude: mechanistic analysis using a computational model *J. Appl. Physiol.* **127** 491–500
Joffre J, Hellman J, Ince C and Ait-Oufella H 2020 Endothelial responses in sepsis *Am. J. Respir. Crit. Care. Med.* **202** 361–70
Karamanoglu M 1997 A system for analysis of arterial blood pressure waveforms in humans *Comput. Biomed. Res.* **30** 244–55
Kelly R, Hayward C, Avolio A and O'Rourke M 1989 Noninvasive determination of age-related changes in the human arterial pulse. *Circulation* **80** 1652–9
Kelly R P, Millasseau S C, Ritter J M and Chowienczyk P J 2001 Vasoactive drugs influence aortic augmentation index independently of pulse-wave velocity in healthy men *Hypertension* **37** 1429–33
Kimmoun A *et al* 2015 β1-adrenergic inhibition improves cardiac and vascular function in experimental septic shock *Crit. Care. Med.* **43** e332–40
Landry D W and Oliver J A 2001 The pathogenesis of vasodilatory shock *N. Engl. J. Med.* **345** 588–95
Li B N, Dong M C and Vai M I 2010 On an automatic delineator for arterial blood pressure waveforms *Biomed. Signal Process. Control* **5** 76–81
Mallat S and Zhong S 1992 Characterization of signals from multiscale edges *IEEE Trans. Pattern. Anal. Mach. Intelligence* **14** 710–32
Manisty C *et al* 2010 Wave reflection predicts cardiovascular events in hypertensive individuals independent of blood pressure and other cardiovascular risk factors. an ascot (Anglo-Scandinavian cardiac outcome trial) substudy *J. Am. Coll. Cardiol.* **56** 24–30
Minhas F U A A and Arif M 2008 Robust electrocardiogram (ECG) beat classification using discrete wavelet transform *Physiol. Meas.* **29** 555–70
Monge García M I *et al* 2018 Noradrenaline modifies arterial reflection phenomena and left ventricular efficiency in septic shock patients: a prospective observational study *J. Crit. Care* **47** 280–6
Morelli A, Egidio A D and Passariello M 2015 Tachycardia in septic shock: pathophysiological implications and pharmacological treatment *Annual Update in Intensive Care and Emergency Medicine* ed J L Vincent (Cham: Springer) (https://doi.org/10.1007/978-3-319-13761-2_9)
Müller-werdan U, Stöckl G and Werdan K 2016 Advances in the management of heart failure: the role of ivabradine *Vasc. Health Risk Manag.* **17** 453–70
Nichols W W, Denardo S J, Wilkinson I B, McEniery C M, Cockcroft J and O'Rourke M F 2008 Effects of arterial stiffness, pulse wave velocity, and wave reflections on the central aortic pressure waveform *J. Clin. Hypertens.* **10** 295–303
Nichols W W, O'Rourke M F and Vlachopoulos C 2011 *McDonald's Blood Flow in Arteries Theoretical, Experimental and Clinical Principles.* (London: CRC Press) 6th edn p 768
Pachauri A and Bhuyan M 2012 Wavelet transform based arterial blood pressure waveform delineator *Int. J. Biol. Biomed. Eng.* **6** 15–25
Pagoulatou S, Adamopoulos D, Rovas G, Bikia V and Stergiopulos N 2021 The effect of left ventricular contractility on arterial hemodynamics: a model-based investigation *PLoS One* **16** 1–14
Pauca A L, Kon N D and O'Rourke M F 2005 Benefit of glyceryl trinitrate on arterial stiffness is directly due to effects on peripheral arteries *Heart* **91** 1428–32
Rudd K E *et al* 2020 Global, regional, and national sepsis incidence and mortality, 1990–2017: analysis for the global burden of disease study *Lancet* **395** 200–11
Rudiger A and Singer M 2013 The heart in sepsis: from basic mechanisms to clinical management *Curr. Vasc. Pharmacol.* **11** 187–95
Sculley D 2010 Web-scale k-means clustering *Proceedings of the 19th International Conference on World Wide Web (Raleigh, North Carolina, USA, April 26-30)* pp 1177–8
Sharman J E, Davies J E, Jenkins C and Marwick T H 2009 Augmentation index, left ventricular contractility, and wave reflection *Hypertension.* **54** 1099–105
Singer M *et al* 2016 The third international consensus definitions for sepsis and septic shock (sepsis-3) *JAMA – J. Am. Med. Assoc.* **315** 801–10
Sun J X, Reisner A T, Mark R G G, Zong W, Moody G B and Mark R G G 2006 A signal abnormality index for arterial blood pressure waveforms *Computers in Cardiology* 2006 *(Valencia, Spain)* 13–16
Vlachopoulos C *et al* 2005 Acute systemic inflammation increases arterial stiffness and decreases wave reflections in healthy individuals *Circulation* **112** 2193–200
Wei C *et al* 2016 Effects of low doses of esmolol on cardiac and vascular function in experimental septic shock *Crit. Care.* **20** 1–10
Westerhof N, Sipkema P, Bos G C V Den and Elzinga G 1972 Forward and backward waves in the arterial system *Cardiovasc Res.* **6** 648–56
Westerhof N and Westerhof B E 2012 Wave transmission and reflection of waves 'The myth is in their use.' *Artery Res.* **6** 1–6
Westerhof N and Westerhof B E 2017 Waves and Windkessels reviewed *Artery Res.* **18** 102–11
Wilkinson I B *et al* 2002 Heart rate dependency of pulse pressure amplification and arterial stiffness *Am. J. Hypertens.* **15** 24–30
Zamani P *et al* 2014 Reflection magnitude as a predictor of mortality the multi-ethnic study of atherosclerosis *Hypertension* **64** 958–64
Zong W, Heldt T, Moody G B and Mark R G 2003 An open-source algorithm to detect onset of arterial blood pressure pulses *Computers in Cardiology* 2003 *(Thessaloniki, Greece)* 259–62